Biochemical Pharmacology, Vol. 57, pp. 1177–1190, 1999.

ISSN 0006-2952/99/$–see front matter
PII S0006-2952(99)00036-2

Functional Analysis of Activation and Repression Domains of the Rainbow Trout Aryl Hydrocarbon Receptor Nuclear Translocator (rtARNT) Protein Isoforms

*Brian Necela and Richard S. Pollenz**

Department of Biochemistry and Molecular Biology, Medical University of South Carolina, Charleston, SC 29425, U.S.A.

ABSTRACT. The aryl hydrocarbon receptor nuclear translocator (ARNT) protein is involved in many signaling pathways. Rainbow trout express isoforms of ARNT protein that are divergent in their C-terminal domains due to alternative RNA splicing. Rainbow trout $ARNT_b$ ($rtARNT_b$) contains a C-terminal domain rich in glutamine and asparagine (QN), whereas the C-terminal domain of $rtARNT_a$ is rich in proline, serine, and threonine (PST). $rtARNT_b$ functions positively in AH receptor-mediated signaling, whereas $rtARNT_a$ functions negatively. Studies were performed to understand how changes in the C-terminal domains of the two rtARNT isoforms affect function. Deletion of the QN-rich C-terminal domain of $rtARNT_b$ did not affect function in aryl hydrocarbon receptor (AHR)-mediated signaling, whereas deletion of the PST-rich domain of $rtARNT_a$ restored function. Expression of the PST-rich domain on truncated $rtARNT_b$ or mouse ARNT (mARNT) reduced function of this protein by 50–80%. Gel shift assays revealed that the PST-rich domain affected AHR-mediated signaling by inhibiting DNA binding of the AHR•ARNT heterodimer. Gal4 transactivation assays revealed a potent transactivation domain in the QN-rich domain of $rtARNT_b$. In contrast, Gal4 proteins containing the PST-rich domain of $rtARNT_a$ did not transactivate because the proteins did not bind to DNA. Secondary structure analysis of the PST-rich domain revealed hydrophilic and hydrophobic regions. Truncation of the hydrophobic domain that spanned the final 20–40 amino acids of the $rtARNT_a$ restored function to the protein, suggesting that repressor function was related to protein misfolding or masking of the basic DNA binding domain. Functional diversity within the C-terminal domain is consistent with other negatively acting transcription factors and illustrates a common biological theme. BIOCHEM PHARMACOL **57**;11: 1177–1190, 1999. © 1999 Elsevier Science Inc.

KEY WORDS. ARNT; AHR; rainbow trout; transactivation; P4501A1; cell culture

The ARNT† protein is a member of the bHLH/PAS family of transcription factors. This family is characterized by the presence of a bHLH motif and a PAS domain, termed for homology among PER, AHR, ARNT, and SIM. The basic region has been shown to be crucial in DNA binding [1–5], whereas the HLH and PAS domains are responsible for dimerization and ligand binding [3, 4, 6]. The bHLH/PAS family includes the AHR, HIF-1α, SIM, PER, and HIF-2α [7–10]. Recently, a new ARNT gene termed *ARNT2* has been identified in mouse and rat [11, 12] as well as alternatively spliced ARNT variants in rainbow trout [13] and humans [14].

ARNT appears to be a dimerization partner for many of the bHLH/PAS proteins. ARNT was first identified in the AHR pathway, mediating the effects of halogenated aromatic hydrocarbons, typified by TCDD [15–17]. In the current model of AHR signal transduction, the AHR is activated by the ligand and then forms a heterodimer with ARNT in the nucleus [18–20]. The AHR•ARNT complex then associates with the XRE to modulate the expression of various genes [5, 21, 22]. In addition, ARNT forms a heterodimer with HIF-1α to regulate hypoxia-inducible genes such as vascular endothelial growth factor, erythropoietin, and numerous glycolytic enzymes and transporters [7, 23–26]. It has also been postulated that ARNT can

* Corresponding author: Dr. Richard S. Pollenz, Department of Biochemistry and Molecular Biology, MUSC, 505BSB, 171 Ashley Ave., Charleston, SC 29425. Tel. (843) 792-4321; FAX (843) 792-4322; E-mail: pollenzr@musc.edu

† *Abbreviations*: ARNT, aryl hydrocarbon receptor nuclear translocator; AHR, aryl hydrocarbon receptor; mAHR, mouse AHR; bHLH, basic helix-loop-helix; rtARNT, rainbow trout ARNT; mARNT, mouse ARNT; hARNT, human ARNT; TCDD, 2,3,7,8-tetrachlorodibenzo-*p*-dioxin; PAS, PER-ARNT-SIM; HIF, hypoxia-inducible factor; GAR-HRP, goat anti-rabbit horseradish peroxidase; GAM-HRP; goat anti-mouse horseradish peroxidase; PER, periodicity; SIM, single minded; TBS, Tris-buffered saline; TTBS, Tris-buffered saline with Tween 20; TBE, Tris, boric acid, EDTA; XRE, xenobiotic response element; DMEM, Dulbecco's minimum essential medium; FBS, fetal bovine serum, PCR, polymerase chain reaction; DTT, dithiothreitol; TAD, transactivation domain; EMSA, electrophoretic mobility shift assay; TNT, transcription and translation; and P450, cytochrome P450.

Received 14 July 1998; accepted 16 October 1998.

function as a homodimer to regulate genes through the CACGTG E-box element [27–29] and can interact with SIM [30–32]. Thus, ARNT appears to be a protein critical to the function of at least three distinct signaling pathways that are activated by different stimuli.

Whereas the bHLH/PAS domains provide the ability of ARNT and other bHLH/PAS proteins to dimerize with each other and bind DNA, the C-terminus may provide domains important for the functional diversity of the various proteins. Indeed, the C-terminal domains of the bHLH/PAS proteins are the least conserved regions of these proteins and are reported to contain domains important for transactivation and repression. Several reports have mapped transcriptional activation domains to the C-terminal end in mARNT, hARNT, ARNT2, HIF-1α, and dSIM [6, 11, 24, 33–37]. In contrast, studies have illustrated that mSIM1 and mSIM2 have a negative impact on ARNT-mediated signaling that is related to the presence of repression domains in the C-terminus [30, 31]. A similar result has been reported for the two ARNT proteins expressed in rainbow trout. $rtARNT_a$ and $rtARNT_b$ are identical proteins over their first 533 amino acids, but each has a distinct C-terminal domain due to the presence or absence of an alternatively spliced exon that also causes a shift in the reading frame [13]. $rtARNT_a$ lacks the exon and has a C-terminal domain of 104 residues rich in proline, serine, and threonine (PST-rich). $rtARNT_b$ contains the exon and has a C-terminal domain of 190 residues rich in glutamine and asparagine (QN-rich). $rtARNT_b$ can complement AHR-mediated signaling when expressed in mouse hepatoma cells that lack functional ARNT protein, whereas $rtARNT_a$ functions inefficiently in the cells and has dominant negative activity over the $rtARNT_b$ protein [13]. Because $rtARNT_a$ is divergent in its C-terminal domain, it is hypothesized that this region must provide some type of repressor functionality to the protein. Collectively, these reports suggest that changes in C-terminal domains of bHLH/PAS proteins may be a mechanism for generating functional diversity.

The experiments in this study were designed to provide new information concerning how changes in the C-terminal domains of rtARNT result in positive and negative function in AHR-mediated signaling. The results indicate that the C-terminal domain of $rtARNT_b$ functions in a manner analogous to that of mammalian ARNT protein and contains a potent transactivation domain. In contrast, the 104-amino-acid PST-rich domain of $rtARNT_a$ is responsible for the negative impact of this protein on AHR-mediated signaling. The addition of this domain to rtARNT and mARNT proteins, whether in the presence or absence of the amino acids encoded by the spliced exon, results in AHR•ARNT complexes that have reduced affinity for DNA and do not complement AHR-mediated signaling in transfected cells. This effect was not specific to the AHR•ARNT complex, as the PST-rich domain also affected the ability of Gal4/rtARNT chimeras to bind DNA. Truncation of 20–40 amino acids from the PST-rich domain relieved the negative impact of this sequence on AHR-mediated signaling and revealed that the truncated domain did not contain potent transactivation function.

MATERIALS AND METHODS

Materials

Specific antibodies against mouse ARNT protein (R-1) and rainbow trout ARNT (rt-84) are identical to those described previously [13, 38]. All antibodies are affinity-purified IgG fractions. Antibodies against Gal4 1–147 (anti-Gal4) were purchased from Santa Cruz Biotechnology. Specific antibodies against the FLAG™ epitope (M5 anti-FLAG™) were purchased from the Kodak Co. For western blot analysis, goat anti-rabbit antibodies or goat anti-mouse antibodies conjugated to horseradish peroxidase (GAR-HRP, GAM-HRP) were utilized. Both of these reagents were purchased from Jackson Immunoresearch. Polyclonal rabbit β-actin antibodies were purchased from the Sigma Chemical Co. Polyclonal rabbit antibodies against mammalian P4501A1 were a gift from Dr. Colin Jefcoate. TCDD was a gift from Monsanto. The reporter plasmid pFR-Luc was purchased from Stratagene.

Buffers

PBS is 0.8% NaCl, 0.02% KCl, 0.14% Na_2HPO_4, 0.02% KH_2PO_4, pH 7.4. 2X gel sample buffer is 125 mM Tris, pH 6.8, 4% SDS, 25% glycerol, 4 mM EDTA, 20 mM DTT, 0.005% bromphenol blue. TBS is 50 mM Tris, 150 mM NaCl, pH 7.5. TTBS is 50 mM Tris, 0.2% Tween 20, 150 mM NaCl, pH 7.5. TTBS+ is 50 mM Tris, 0.5% Tween 20, 300 mM NaCl, pH 7.5. BLOTTO is 5% dry milk in TTBS. 2× lysis buffer is 50 mM HEPES, pH 7.4, 40 mM sodium molybdate, 10 mM EGTA, 6 mM $MgCl_2$, 20% glycerol. 5× gel shift buffer is 50 mM HEPES, pH 7.5, 15 mM $MgCl_2$, 50% glycerol. 0.5× TBE is 45 mM Tris-borate, 1 mM EDTA. MENG is 10 mM MOPS, 5 mM EDTA, 0.02% NaN_3, 10% glycerol.

Oligonucleotides

All primers are written 5′–3′. Restriction sites are underlined. ATG start codons and TTA stop codons are in boldface.

Primer 1, TATAAAGCTTTGATCACC**ATG**GCGG CGACTACAGCT;

Primer 2, TATATCTAGAGGACAGTTCCAGGCCC GGTGT;

Primer 3, TATAGGATCCCCTGTTGGGTGGCAG GGACAGT;

Primer 4, TATAGAATTCTGTGGTCTGTCCAGTCT CAGGAG;

Primer 5, TATAGAATTC**ATG**GACTCTTCTATCC CAGAC;

Primer 6, TATATCTAGACGATAA**TTA**GACATG CTCTCTTTG;

Primer 7, TATATCTAGA**TTA**GCTGTATGTGTC GTTGGAGC;
Primer 8, TATATCTAGA**TTA**CTGCTGCCCCGA CCCCAAGCC;
Primer 9, TATAGAATTCTCAGTAGGG**ATG**GCCC CTCAG;
Primer 10, TATAGGATCCTAGGG**ATG**GCCCCTC AGATG;
Primer 11, TATAGAATTCTCCCCTCCAGGGCAGT GGAG;
Primer 12, TATAGAATTCCCCTCCAGGGCAGT GGAG;
Primer 13, TATATCTAGA**TTA**CTGGCTGGTCC AGCATGGCGA;
Primer 14, TATATCTAGA**TTA**GAGAGAAGGAG ACATTTGAGA;
Primer 15, TATAGAATTCGGCACC**ATG**GACTA CAAGGACGACGATGACAAAGACCTTCTATCCC AGACATACCA;
Primer 16, TATAGAATTCGGCACC**ATG**GACTA CAAGGACGACGATGACAAAGCGGCGACTACAG CTAACCCAGAA;
XRE-1, CGGCTCGGAGTTGCGTGAGAAGAG;
XRE-2, CGGCTCTTCTCACGCAACTCCGAG;
GAL4BS, ACTGCTCGGAGGACAGTACTCCGCT;

Cells and Growth Conditions

Type II Hepa-1 variants were a gift from Dr. Jim Whitlock, Jr. The cells were propagated at 37° in DMEM medium containing 5% FBS. All cells were passaged at 1-week intervals and used in experiments during a 2-month period.

Plasmid Construction

A mammalian Gal4 fusion expression vector was generated as follows. A *Hin*dIII-*Xba*I fragment corresponding to the Gal4 DNA binding domain (amino acids 1–147) was excised from the plasmid psg424 [39] and ligated into pcDNA3.1 (Invitrogen) to generate pc424. This vector contains the Gal4 DNA binding domain upstream of a new multicloning site and is under the control of a CMV promoter. The multicloning site contains *Eco*RI, *Bam*HI, and *Xba*I restriction sites for the in-frame ligation of cDNAs immediately downstream of Gal4 1–147.

Generation of mARNT cDNAs and Expression Vectors

All mouse constructs were amplified by PCR using the plasmid pMVmARNT as a template. Primer 1 and primer 2 were used to amplify a 2166-bp *Hin*dIII-*Xba*I fragment corresponding to full-length mARNT. The 1749-bp *Hin*dIII-*Bam*HI fragment, $mARNT_{583}$, was amplified using primer 1 and primer 3. To amplify the $mARNT_{583}$ with *Hin*dIII-*Eco*RI sites, primer 1 and primer 4 were utilized. All PCR products were digested and ligated into pcDNA3.1. These plasmids are referred to by the prefix "pc" followed by the name of the construct. mARNT/rtARNT chimeras were generated as follows. Primer 10 and primer 6 were used to amplify a 708-bp *Bam*HI-*Xba*I fragment, $rtARNT_{EX\text{-}PST}$, from the plasmid $pMVrtARNT_{b\text{-}a}$. The 708-bp *Eco*RI-*Xba*I fragment, $rtARNT_{EX\text{-}QN}$, was amplified using primer 9 and primer 6 from $pMVrtARNT_b$. The expression construct $pcmARNT_{583\text{-}rtEX\text{-}PST}$ was generated by ligating the $rtARNT_{EX\text{-}PST}$ fragment into the *Bam*HI-*Xba*I sites of $pcmARNT_{583}$. The $rtARNT_{EX\text{-}QN}$ fragment was ligated into the *Eco*RI-*Xba*I sites of $pcmARNT_{583}$ to create $pcmARNT_{583\text{-}rtEX\text{-}QN}$. To incorporate the eight-amino-acid tag, FLAG™, into the 5′ end of mARNT, primer 15 and primer 2 were used to amplify from pMVmARNT.

Generation of rtARNT cDNAs and Expression Vectors

PCR was used to amplify fragments of rtARNT from the plasmids $pMVrtARNT_a$, $pMVrtARNT_b$, and $pMVrtARNT_{b\text{-}a}$ [13]. All constructs contain *Eco*RI-*Xba*I restriction sites, except for $rtARNT_{EX\text{-}PST,}$ which has a *Bam*HI-*Xba*I site. Primer 5 and primer 6 were used to amplify the full-length $rtARNT_a$ (1936 bp) and $rtARNT_b$ (2306 bp) from $pMVrtARNT_a$ and $pMVrtARNT_b$. Primer 5 and primer 7 were used to amplify a 1601-bp fragment, $rtARNT_{533,}$ from $pMVrtARNT_b$. $rtARNT_{533\text{-}EX}$ was generated using primer 5 and primer 8 with $pCMVrtARNT_b$ as a template. Primer 9 and primer 6 were used to amplify a 708-bp fragment, $rtARNT_{EX\text{-}QN}$, from rtARNT. The 708-bp *Bam*HI-*Xba*I fragment, $rtARNT_{EX\text{-}PST}$, was amplified from $pMVrtARNT_{b\text{-}a}$ with primer 10 and primer 6. The COOH end of $rtARNT_a$, $rtARNT_{PST}$, was amplified using primer 14 and primer 6 with $pMVrtARNT_a$ as a template. Primer 12 and primer 6 were used to amplify the 335-bp COOH end of $rtARNT_b$ ($rtARNT_{QN}$) from $pMVrtARNT_b$. The 373-bp exon of $rtARNT_b$, $rtARNT_{EX}$, was amplified from $pMVrtARNT_b$ with primer 9 and primer 8. To generate $rtARNT_{\Delta 580}$, primer 5 and primer 13 were used to amplify the fragment from $pMVrtARNT_b$. Primer 5 and primer 14 were used to amplify the fragment $rtARNT_{\Delta 617}$ from $pMVrtARNT_b$. The FLAG™ epitope was incorporated into the 5′ end of $rtARNT_b$, creating FLAG™-$rtARNT_b$, by amplifying from $pMVrtARNT_b$ with primer 16 and primer 2. For generation of Gal4/rtARNT fusions, the rtARNT fragments were digested and ligated into pc424, immediately downstream of the Gal4 DNA binding domain. For complementation studies, rtARNT fragments were inserted into the multi-cloning site of pcDNA3.1. All constructs were ligated in *Eco*RI-*Xba*I sites except for $rtARNT_{EX\text{-}PST}$, which was inserted into the *Bam*HI-*Xba*I site.

Nucleotide and Amino Acid Analysis

PCR products were sequenced using the ABI 377 automated DNA sequencer (Applied Biosystems). Prediction of the secondary structure of $rtARNT_a$ was performed using Lasergene software (DNASTAR). Analysis of the amino

acid sequence of $rtARNT_a$ for protein kinase sites was done using the MOTIF database (ICR).

In Vitro *Expression of ARNT Proteins*

The recombinant rtARNT and mARNT proteins were produced using the TNT™ Coupled Rabbit Reticulocyte Lysate System, and the Gal4/rtARNT proteins were produced using the Wheat Germ Extract Kit essentially as detailed by the manufacturer (Promega). Upon completion of the 90-min reaction, samples were either combined with an equal volume of 2X gel sample buffer and boiled for 5 min, or stored at −20° for use in functional studies. The actual concentration of each recombinant protein expressed in each reaction was determined by western blot analysis with the R-1, rt-84, anti-Gal4, or M5 anti-FLAG™ antibody. Generally, 1–5 μL of TNT reaction was used for functional studies and 1–5 μL of the denatured TNT for western blotting.

Eukaryotic Transfections and Reporter Gene Assays

Approximately 5×10^5 type II cells were plated into 60-mm culture dishes and incubated at 37° for 16–24 hr. Then 1–2 μg of appropriate plasmid vectors were transfected into cells with LipofectAMINE™ as detailed by the manufacturer (Gibco). For complementation studies, after a 24-hr recovery cells were incubated in the presence of 2 nM TCDD or DMSO for an additional 20–40 hr. Cells were harvested from plates by trypsinization, and total cell lysates were prepared as detailed below. For transactivation studies, the cells were also transfected with 1.0 μg of the reporter gene pFR-Luc and 1.0 μg of pSV-β-galactosidase to monitor transfection efficiency (Promega). Cells were harvested 24–48 hr after transfection. In these instances, harvested cells were split into two equal fractions. One fraction was used for the preparation of total lysates. The other fraction was resuspended in reporter lysis buffer (Promega), and β-gal and luciferase activities were determined as detailed by the manufacturer (Promega). Three, four, or five plates were transfected with each plasmid being evaluated, and experiments were completed three times.

Production of Total Cell Lysates and Cytosol

Total cell lysates for western blot analysis were prepared by sonicating cell pellets in 1X lysis buffer and NP-40 as detailed previously [18, 38]. Cytosol was prepared from type II Hepa-1 cells by homogenization in MENG buffer supplemented with leupeptin (10 μg/mL), aprotinin (20 μg/mL), and phenylmethylsulfonyl fluoride (PMSF) (100 μM). Homogenates were centrifuged at 22,000 *g* in a refrigerated microcentrifuge, and aliquots of the supernatant were stored at −70° prior to use in EMSA and immunoprecipitation studies. Protein concentrations were determined by the Coomassie Blue Plus assay (Pierce) using BSA as the standard.

Western Blot Analysis and Quantification of Protein

Protein samples were resolved by denaturing electrophoresis on discontinuous polyacrylamide slab gels (SDS–PAGE) and were electrophoretically transferred to nitrocellulose as described [38, 40]. Immunochemical staining was carried out with various concentrations of primary antibody (see text and figure legends) in BLOTTO buffer supplemented with DL-histidine (20 mM) for 1–2 hr at 22°. Blots were washed with three changes of TTBS+ for a total of 45 min. The blot was then incubated in BLOTTO buffer containing a 1:10,000 dilution of GAR-HRP or GAM-HRP (see text and figure legends) for 1 hr at 22° and washed in three changes of TTBS+ as above. Prior to detection, the blots were washed in TBS for 5 min. Bands were visualized with the enhanced chemiluminescence (ECL) kit as specified by the manufacturer (Amersham). Multiple exposures of each set of samples were produced. The relative concentrations of rtARNT, P4501A1, and actin were determined by computer analysis of the autoradiographs as detailed previously [18, 19]. Then the values for P4501A1 were divided by the level of ARNT protein. All exposures analyzed by this method were within the linear range established for each antibody [18, 19]. In most instances, the mean and standard deviation of at least three independent samples are reported.

In Vitro *Activation of AHR•ARNT Complexes and EMSA*

AHR•ARNT complexes were produced by combining approximately 50–80 ng of *in vitro* translated mARNT or rtARNT proteins with 100 μg of type II cytosol in the presence of 10 nM TCDD or 0.5% DMSO at 30° for 2 hr. The amount of each recombinant protein added to each sample was always identical, as determined by western blotting of the input protein (as detailed above). Samples were used immediately or stored at −70°.

Oligonucleotides XRE-1 and XRE-2 were annealed and labeled with [^{32}P]dCTP by Klenow fill-in [40]. The double-stranded fragment corresponds to the consensus XRE-1 of the *CYP1A1* promoter as previously described [41]. Next 10–20 μg of nuclear extract or *in vitro* activated type II cytosol was incubated at 22° for 15 min in 1X gel shift buffer supplemented with KCl (80 mM) and poly(dI-dC) (0.1 mg/mL). In some instances, 0.5 to 1.0 μg of affinity-purified R-1, rt-84, A-1, or preimmune IgG was included in the sample. Approximately 4 ng of ^{32}P-labeled XRE then was added to each sample, and the incubation continued for an additional 15 min at 22°. The samples were resolved on 5% acrylamide/0.5× TBE gels, dried, and exposed to film. Specific bands were quantified by computer densitometry as detailed for protein [18]. The bands were not normalized to the level of input ARNT protein.

EMSA of Gal4/rtARNT Proteins

Oligonucleotide Gal4BS was annealed and labeled with [^{32}P]dATP. The double-stranded fragment corresponds to the consensus Gal4 binding site [42, 43]. The desired *in vitro* expressed Gal4/rtARNT protein was incubated at 22° for 15 min in 1× gel shift buffer supplemented with KCl (120 mM) and poly(dI-dC) (0.1 mg/mL). In some instances, 0.5 to 1.0 μg of affinity-purified anti-Gal4 antibody was included in the sample. Then approximately 4 ng of ^{32}P-labeled XRE was added to each sample, and the incubation continued for an additional 15 min at 22°. The samples were resolved on 5% acrylamide/0.5× TBE gels, dried, and exposed to film. Specific bands were quantified by computer densitometry as detailed for protein [18]. The bands were not normalized to the level of input Gal4/rtARNT protein.

RESULTS AND DISCUSSION

Ability of rtARNT$_b$ and mARNT to Complement AHR-Mediated Signaling

The strategy of the studies in this report was to evaluate the ability of various rtARNT isoforms to complement AHR-mediated signal transduction in the type II Hepa-1 cell line. The choice of a mammalian cell line for analysis of rtARNT was due to (i) the fact that type II cells do not express high levels of mARNT, (ii) the ability to assay the expression of recombinant rtARNT protein in total cell lysates, (iii) the ability to evaluate complementation of AHR-mediated signaling by analysis of endogenous P4501A1 protein, and (iv) lack of an appropriate aquatic cell culture model. It is important therefore, to understand whether rtARNT and mARNT complement AHR-mediated signaling to the same level. To address this issue, it was first necessary to titer the antibodies that recognize rtARNT and mARNT since they have different sensitivities.

Expression vectors were constructed so that the FLAG™ peptide was expressed at the NH-terminus of rtARNT$_b$ and mARNT proteins. The proteins were then expressed *in vitro*, and equal amounts of sample were evaluated by western blotting with anti-FLAG™ antibodies. Figure 1A shows that the amount of FLAG™-rtARNT$_b$ and FLAG™-mARNT protein present in the lysates was within 8%. Identical blots then were stained with antibodies against rtARNT (rt-84, 1.0 μg/mL) or mARNT (R-1, 0.2 μg/mL). Figure 1A shows that these dilutions of antibody detected a similar level of FLAG™-rtARNT$_b$ and FLAG™-mARNT protein and are consistent with the sensitivity of these reagents [13, 19]. rtARNT$_b$ and mARNT expression vectors then were transfected into type II cells, treated with TCDD, and equal concentrations of whole cell lysates were evaluated on western blots with the antibody concentrations detailed above. The results show that the level of mARNT and rtARNT$_b$ protein expression and induction of endogenous P4501A1 protein in the transfected cells was within 10%. Importantly, P4501A1 protein was not detected in cells that were not exposed to TCDD (data not shown). The difference in apparent molecular mass of mARNT in panels A and B reflects the use of different percentage SDS–PAGE gels in these experiments. These results suggest that rtARNT$_b$ is able to function in concert with mAHR to the same level of efficiency as mARNT and indicates that the Hepa-1 type II cell is an appropriate model to evaluate rtARNT function. These results are consistent with the finding that rtARNT$_b$ and mARNT share > 80% amino acid sequence identity over the NH-terminal 533 amino acids with 100% amino acid conservation in the bHLH domain [13], and that AHR-mediated signal transduction is similar in mammalian and aquatic cells [44].

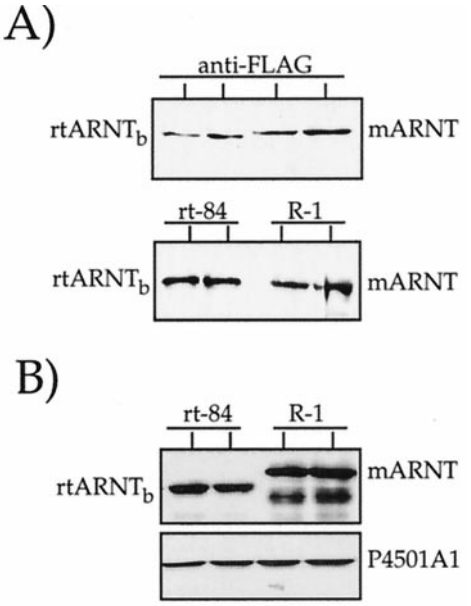

FIG. 1. Comparison of rtARNT$_b$ and mARNT function in type II Hepa-1 cells. (A) Titer of antibodies against rtARNT$_b$ and mARNT. rtARNT$_b$ and mARNT proteins containing the FLAG™ peptide were produced in a coupled TNT reaction, subjected to denaturing gel electrophoresis, and blotted to nitrocellulose. Half the blot was stained with anti-FLAG™ antibody followed by GAM-HRP (1:10,000) to determine whether the proteins were expressed to the same level. The other half was stained with rt-84 IgG (1 μg/mL) or R-1 IgG (0.2 μg/mL) followed by GAR-HRP (1:10,000). The blots were visualized by ECL. Note that these concentrations of antibody resulted in similar levels of reactivity. (B) Western blot of P4501A1 expression in TCDD-treated type II cells expressing rtARNT$_b$ and mARNT protein. Two plates of type II cells were transfected with rtARNT$_b$ or mARNT, treated with TCDD (1 nM) for 16 hr, and total cell lysates were prepared. Eighteen micrograms of each sample was subjected to denaturing gel electrophoresis and blotted to nitrocellulose. The blot was stained with either rt-84 IgG (1.0 μg/mL) or R-1 IgG (0.2 μg/mL), and a duplicate blot was stained with anti-P4501A1 IgG (1:500). Blots were then stained with GAR-HRP (1:10,000) and visualized by ECL.

Analysis of PST-Rich C-Terminal Domain

rtARNT$_a$ contains a 104-amino-acid PST-rich C-terminal domain and is also missing 123 amino acids encoded by an

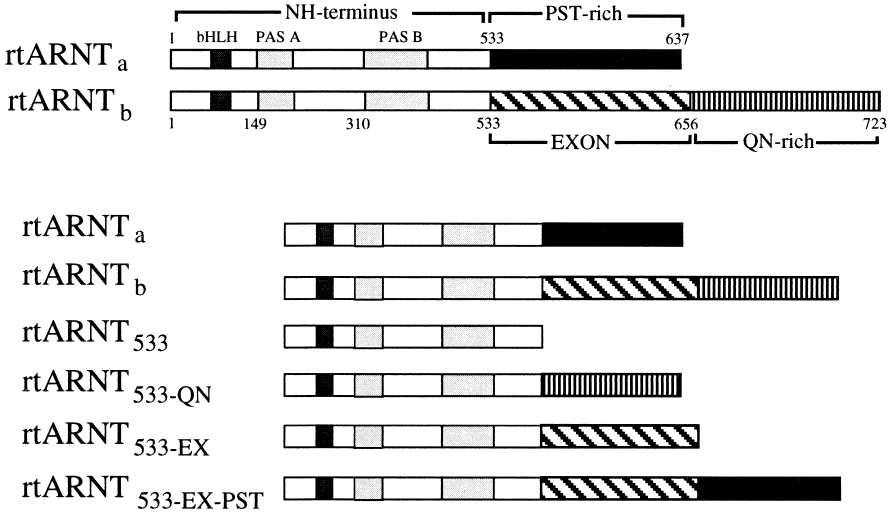

FIG. 2. Schematic diagram of rtARNT$_a$ and rtARNT$_b$ showing the structure of C-terminal constructs. All constructs were ligated into pcDNA3.1 for expression *in vivo* and *in vitro*. Numbers indicate amino acids. Specific domains are indicated.

alternatively spliced exon [13]. Since rtARNT$_a$ has dominant negative activity in AHR-mediated signaling, it has been hypothesized that the divergent C-terminal region must provide some type of repressor function to the protein. It is unclear, however, whether the repressor function is related to the presence of the PST-rich C-terminal domain, lack of the 123 amino acids encoded by the exon, or both. It is also unclear how the C-terminal domain affects function at the N-terminus. To begin to investigate these questions, chimeric and truncated rtARNT proteins were evaluated for their ability to complement endogenous AHR-mediated signaling in ARNT-defective cells. A schematic representation of the rtARNT$_a$ and rtARNT$_b$ protein domains and the constructs used to express the chimeric proteins is shown in Fig. 2.

Type II cells were transfected with identical amounts of each construct shown in Fig. 2, treated with TCDD (2 nM), and processed as detailed in Materials and Methods. The levels of rtARNT and P4501A1 protein were then determined by western blotting and quantified by computer densitometry. Figure 3A shows a representative blot, with each lane representing a single plate of cells. The results show that all of the transfected cells expressed a similar level of rtARNT protein that migrated at the expected molecular mass. Following TCDD treatment, cells transfected with rtARNT$_b$, rtARNT$_{533\text{-}EX}$, rtARNT$_{533}$, and rtARNT$_{533\text{-}QN}$ expressed detectable levels of P4501A1. In contrast, expression of rtARNT$_a$ did not result in high levels of P4501A1 induction in type II cells following treatment with TCDD. Figure 3C shows the results for P4501A1 expression normalized to the level of rtARNT protein expression and presented as the percentage of expression compared with rtARNT$_b$. Importantly, removal of the 123-amino-acid region encoded by the exon from rtARNT$_b$ resulted in a protein (rtARNT$_{533\text{-}QN}$) that could complement AHR-mediated signaling to 80% of rtARNT$_b$. In addition, the expression of the 104-amino-acid PST-rich domain on the C-terminus of rtARNT$_{533\text{-}EX}$ (rtARNT$_{533\text{-}EX\text{-}PST}$) reduced the level of TCDD-inducible P4501A1 protein by > 90% (Fig. 3, A and C).

These results indicate that deletion of the 67-amino-acid QN-rich domain from rtARNT$_b$ has a minimal effect on AHR-mediated signaling. However, deletion of the 123-amino-acid domain encoded by the exon affected AHR-mediated signaling by 25–50%. This suggests that rtARNT$_b$ can function independently of its C-terminus in AHR-mediated signaling but that more extensive deletions affect protein function. These results are consistent with previous studies that have evaluated the function of the C-terminus of mammalian ARNT *in vitro* and *in vivo* [34, 45]. The finding that removal of the PST-rich domain from rtARNT$_a$ (rtARNT$_{533}$) restores functionality to rtARNT, and that rtARNT$_{533\text{-}QN}$ is also highly functional, indicates that the PST-rich domain is solely responsible for the negative function of rtARNT$_a$ on AHR-mediated signaling and that the 123 amino acids encoded by the exon do not contribute to this function. This hypothesis is further supported by the finding that addition of the PST-rich domain to rtARNT$_{533\text{-}EX}$ (rtARNT$_{533\text{-}EX\text{-}PST}$) results in a protein that functions in a manner similar to that of rtARNT$_a$.

PST-Rich C-Terminal Domain and XRE Binding

The reduction in TCDD-induced expression of P4501A1 in type II cells expressing rtARNT$_{533\text{-}EX\text{-}PST}$ could be the result of inefficient formation of rtARNT•AHR complexes, decreased affinity of the rtARNT•AHR complex for DNA, or repression of the transactivation supplied by the AHR. Studies focused on the association of the rtARNT•mAHR complex with DNA, since previous results showed that rtARNT$_a$ formed dimers with mAHR [13]. To evaluate the interaction of the various rtARNT•mAHR complexes with DNA, rtARNT protein

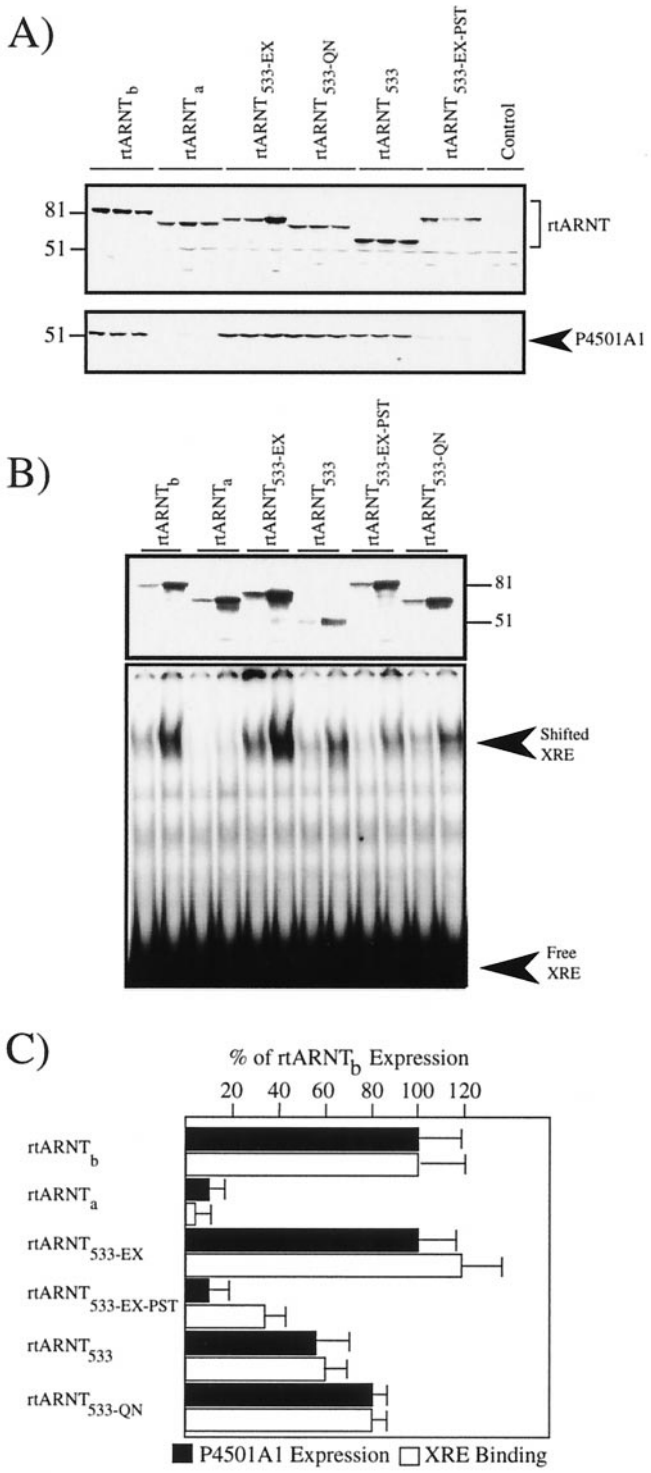

FIG. 3. Analysis of C-terminal domains of rtARNT$_a$ and rtARNT$_b$. (A) Western blot of P4501A1 expression in TCDD-treated type II cells expressing rtARNT proteins. Three plates of type II cells were transfected with the indicated constructs, treated with TCDD (1 nM) for 16 hr, and total cell lysates were prepared. Eighteen micrograms of each sample was subjected to denaturing gel electrophoresis and blotted to nitrocellulose. Duplicate blots were stained with either rt-84 IgG (1.0 μg/mL) or anti-P4501A1 IgG (1:500). Blots then were stained with GAR-HRP (1:10,000) and visualized by ECL. (B) EMSA of rtARNT protein. One hundred micrograms of type II cytosol was combined with either 20 or 50 ng of the indicated rtARNT protein. Then samples were activated with TCDD (10 nM) for 2 hr at 30°, and EMSA was performed as detailed in Materials and Methods. The specifically shifted band associated with rtARNT•AHR•XRE complex is indicated. The western blot at the top of the EMSA represents an aliquot of the exact samples used for the EMSA stained with the rt-84 antibody as detailed in part A. Each pair of lanes represents use of 20 and 50 ng of the indicated ARNT protein, respectively. Molecular mass markers were BSA (81 kDa) and ovalbumin (51 kDa). (C) Composite of P4501A1 expression and XRE binding. The levels of P4501A1, rtARNT protein, and specifically shifted XRE were quantified by computer densitometry as detailed in Materials and Methods. These data are presented as the percentage of P4501A1 expression or XRE binding compared with rtARNT$_b$ (100%). Each bar represents the mean ± range of two independent experiments, of which the data from 3B (50 ng lanes) represents one.

was produced *in vitro* and quantified on western blots. Identical amounts of recombinant protein were then combined with type II cytosol and activated with TCDD at 30° for 2 hr. The formation of functional rtARNT•mAHR complexes was then evaluated by EMSA using an oligonucleotide containing the putative XRE sequence [41]. An aliquot of the identical sample used for the EMSA was also evaluated for the level of input rtARNT by western blotting. Figure 3B shows the results of a typical assay. It can be observed that the level of input rtARNT protein is consistent for all samples. Samples containing rtARNT$_b$ and type II cytosol were able to shift the putative XRE following TCDD activation. In addition, a strong shift was observed with rtARNT$_{533\text{-}EX}$, and a shift was also detected with rtARNT$_{533}$ and rtARNT$_{533\text{-}QN}$. In contrast, when the PST-rich C-terminal domain was present on the expressed protein (rtARNT$_a$ or rtARNT$_{533\text{-}EX\text{-}PST}$), a minimal shift was observed. The specifically shifted bands were quantified by computer densitometry, and the data are presented as the percentage of expression compared with rtARNT$_b$ (Fig. 3C). The data directly parallel the results from the complementation experiments and suggest that the reduced function of proteins containing the PST-rich domain is at the level of DNA binding. In addition, reductions in functionality of rtARNT$_b$ due to C-terminal deletions are at the level of DNA binding. This hypothesis is supported by immunoprecipitation experiments that showed that all of the rtARNT chimeric proteins associated with the mAHR (data not shown).

Having established that the PST-rich C-terminal domain of rtARNT$_a$ was responsible for the divergent function of this protein, it was of interest to determine whether this domain would have similar functions in the context of the mARNT protein. rtARNT and mARNT amino acid sequences were aligned, and this established that truncation of the C-terminal 205 amino acids of mARNT (mARNT$_{583}$) would be the correlate to the rtARNT$_{533}$. The rtEX-PST and rtEX-QN sequences were then ligated to mARNT$_{583}$ so that function could be analyzed. The various ARNT chimeras are illustrated in Fig. 4A. Each chimeric protein was expressed *in vitro* and quantified by western blotting with the R-1 antibody. However, since the

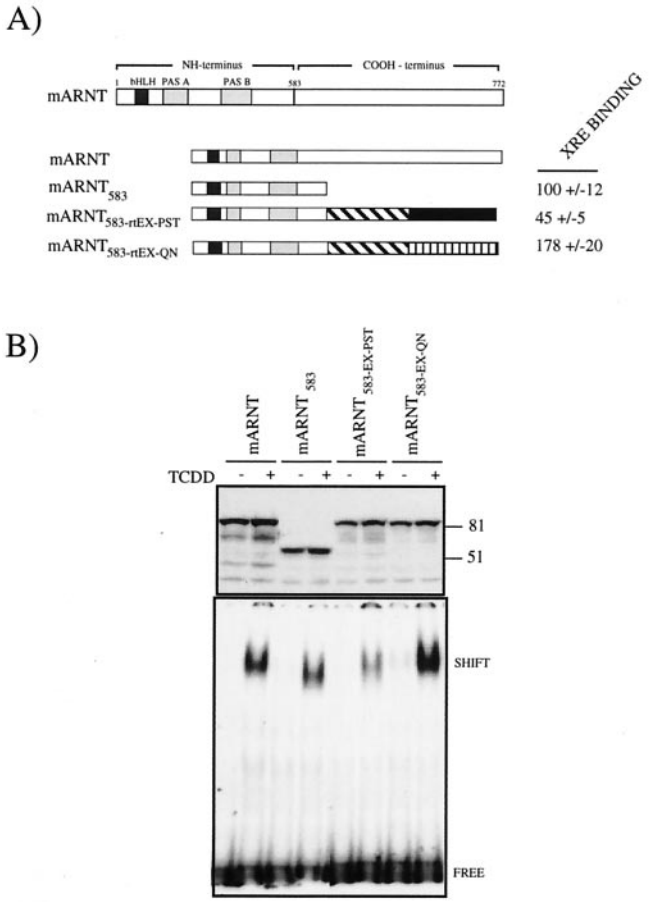

FIG. 4. Analysis of C-terminal domains of rtARNT$_a$ and rtARNT$_b$ in the context of mARNT. (A) Schematic diagram of mARNT and structure of rtARNT/mARNT chimeras. All constructs were ligated into pcDNA3.1 for expression *in vivo* and *in vitro*. (B) EMSA of mARNT chimeric protein. One hundred micrograms of type II cytosol was combined with 50 ng of the indicated mARNT protein. Then samples were activated with TCDD (10 nM) for 2 hr at 30°, and EMSA was performed as detailed in Materials and Methods. The specifically shifted band associated with ARNT•AHR•XRE complex is indicated. The western blot at the top of the EMSA represents an aliquot of the exact samples used for the EMSA stained with the R-1 antibody as detailed in Materials and Methods. Molecular mass markers were BSA (81 kDa) and ovalbumin (51 kDa).

R-1 antibody was produced against the C-terminal half of mARNT [38], and this portion of the protein is truncated, the level of chimeric protein cannot be compared to the level of full-length mARNT, and thus mARNT is included as a positive control. To evaluate function, identical amounts of mARNT$_{583}$, mARNT$_{rtEX-QN}$, and mARNT$_{rtEX-PST}$ were combined with type II cytosol, activated with TCDD, and EMSA was performed as described. Figure 4B shows the results of a representative assay. The western blots of the exact samples used in the gel shift assay are also shown in Fig. 4B.

Type II cytosol supplemented with mARNT and activated with TCDD showed a strong shift, and served as a positive control. mARNT$_{583}$ was also capable of forming mARNT•AHR complexes that bound the XRE as observed for rtARNT$_{533}$. When the rtEX-QN domain was added to the mARNT$_{583}$ (mARNT$_{583\text{-}rtEX\text{-}QN}$), the intensity of the gel shift was increased by 78%. In contrast, addition of the rtEX-PST region to mARNT$_{583}$ (mARNT$_{rtEX\text{-}PST}$) resulted in a > 50% reduction in binding at the XRE, which was approximately 25% of the level observed with the mARNT$_{rtEX\text{-}QN}$ protein. Experiments confirmed that all mARNT chimeras associate with the mAHR and that mARNT$_{rtEX\text{-}QN}$ but not mARNT$_{rtEX\text{-}PST}$ complemented AHR-mediated signaling in type II cells (data not shown). Collectively, these findings support the hypothesis that the PST-rich C-terminal domain is responsible for the reduced function of rtARNT$_a$ and indicate that the domain can affect mammalian proteins.

Transactivation Potential of rtARNT$_b$ and rtARNT$_a$

Since ARNT functions in numerous signal transduction pathways, it was of interest to investigate whether the rtARNT$_a$ and rtARNT$_b$ proteins contained TADs. Previous studies have shown the presence of TADs in the C-terminal portion of mammalian ARNT and other bHLH proteins [6, 11, 24, 33–37]. In addition, sequences rich in proline, serine, and threonine have been shown to contain transactivation function. To begin to address this question, the standard Gal4 assay system was utilized [39]. Gal4/rtARNT chimeras were generated by ligating the exon (EX) and C-terminal regions of rtARNT$_a$ (PST) and rtARNT$_b$ (QN) to the Gal4 DNA binding domain (Fig. 5A). Each Gal4/rtARNT chimera was expressed *in vitro* and quantified by western blotting using an antibody against the Gal4 1–147 sequence (data not shown). All proteins migrated at the correct molecular mass and appeared to be expressed to a similar level *in vitro*.

To evaluate the transcriptional activity of the chimeric proteins, each construct was cotransfected into the type II Hepa-1 cell line with the reporter gene, pFR-LUC, and pSVβ-galactosidase. Luciferase assays were performed and cell lysates prepared as detailed in Materials and Methods. In addition, equal amounts of each lysate were resolved by SDS–PAGE, transferred to nitrocellulose, and evaluated for expression of the Gal4/rtARNT chimeras with the anti-Gal4 antibody. It was anticipated that the luciferase activity could be normalized to the level of expressed protein and not transfection efficiency, just as was done for the analysis of P4501A1 induction. Unfortunately, the anti-Gal4 antibody showed a high level of cross-reactivity with type II lysate, making quantification of protein expression unreliable. Thus, the transcriptional activity for each construct could not be normalized to protein expression and was calculated by dividing the luciferase activity by transfection efficiency. Figure 5A shows the normalized values for the various Gal4/rtARNT proteins.

The results indicate that proteins containing the QN domain of rtARNT$_b$ induced high levels of luciferase activity. This observation suggests the presence of a potent TAD in the C-terminal region of rtARNT$_b$. In addition, it

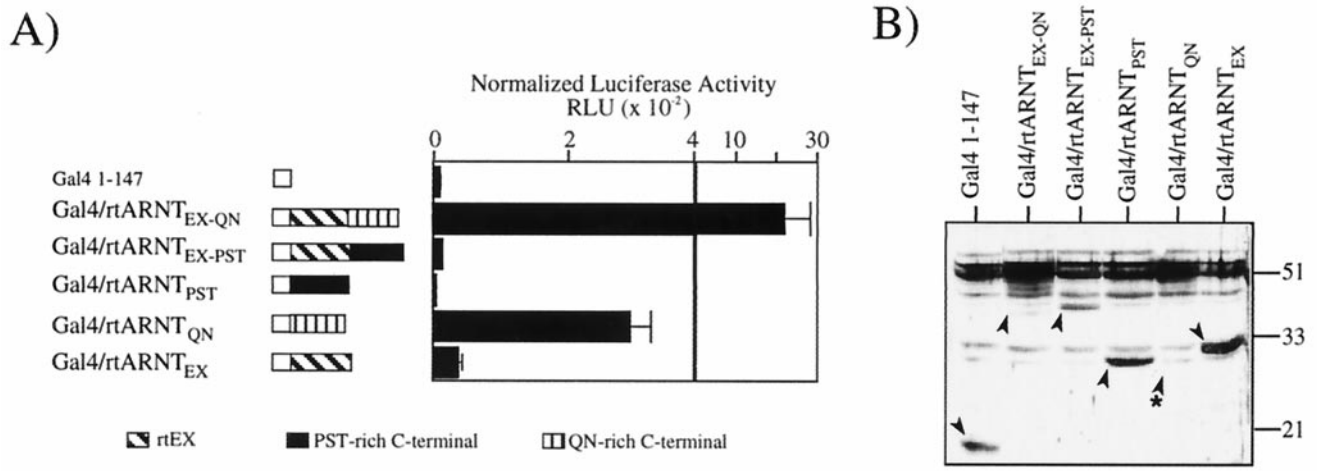

FIG. 5. Analysis of transactivation domains within C-terminal regions of rtARNT$_a$ and rtARNT$_b$. (A) The indicated C-terminal domains of rtARNT$_a$ and rtARNT$_b$ were ligated to the Gal4 DNA binding domain (refer to Fig. 2 for details of the rtARNT domains). The indicated constructs were co-transfected into 3–6 plates of type II cells with a luciferase reporter vector (pFR-LUC) and a β-galactosidase expression vector (pSV-β-gal). Cells were harvested by trypsinization and split into two equal fractions. One fraction was analyzed for luciferase and β-galactosidase activity as detailed in Materials and Methods. The other fraction was used to generate total cell lysates for analysis of Gal4/rtARNT protein expression (below). Then the level of luciferase activity was divided by the level of β-gal activity to normalize for transfection efficiency. Normalized luciferase activity values are means ± SD of 3–6 samples. (B) Western blot analysis of Gal4/rtARNT protein expression. To correlate the luciferase activity to the level of Gal4/rtARNT protein expression, 18 μg of total cell lysate from the indicated samples was subjected to denaturing gel electrophoresis and blotted to nitrocellulose. The blot was stained with anti-Gal4 antibody (Santa Cruz Biotechnology) followed by GAR-HRP (1:10,000) and visualized by ECL. Arrowheads indicate the location of each Gal4/rtARNT protein. An arrowhead with an asterisk indicates the expected location of Gal4/rtARNT$_{QN}$, which despite low expression showed the highest level of transactivation activity. Molecular mass markers were ovalbumin (51 kDa), carbonic anhydrase (33 kDa), and lysozyme (21 kDa).

appears that the 123-amino-acid domain expressed from the exon (i.e. Gal4/rtARNT$_{EX}$) harbored weak transcriptional activity that in combination with the QN region increased transcriptional activity by 20-fold. These results are consistent with reports that have mapped TAD domains within the C-terminal region of mammalian ARNT and AHR [6, 33–36]. However, because the levels of expression of Gal4/rtARNT$_{QN}$ and Gal4/rtARNT$_{EX-QN}$ protein were so different (Fig. 5B), it is not clear whether Gal4/rtARNT$_{EX-QN}$ is truly more active than Gal4/rtARNT$_{QN}$.

Unexpectedly, the C-terminal PST region of rtARNT$_a$ did not exhibit transcriptional activity in the Gal4 assay. In addition, the activity of the Gal4/rtARNT$_{EX-PST}$ was actually 3-fold lower than that of the Gal4/rtARNT$_{EX}$ alone. These data are consistent with the complementation experiments where the addition of the PST domain to rtARNT$_{EX}$ reduced the function of the protein in AHR-mediated signaling. Importantly, the lack of transcriptional activity of Gal4 constructs containing the PST-rich domain cannot be due to reduced expression of these chimeric proteins, as they were highly expressed in transfected cells (Fig. 5B). Thus, these results suggest that despite the presence of serine, threonine, and proline residues, the C-terminal region of rtARNT$_a$ does not harbor TADs. Alternatively, these Gal4 chimeras may not associate with DNA.

Since the PST-rich domain of rtARNT$_a$ produced a negative effect on the DNA binding of the ARNT•AHR complex (Figs. 3 and 4), the lack of transcriptional activity of Gal4 constructs containing the PST-rich domain also could be due to the failure of these proteins to associate with the Gal4 DNA. To address this issue, each Gal4/rtARNT construct was expressed *in vitro*, and the relative concentration of each protein was determined by western blotting. The ability of each recombinant protein to bind DNA then was evaluated by EMSA using an oligonucleotide containing the Gal4 binding site sequence 5′-CGGAGGACAGTACTCCG-3′ [42, 43]. Figure 6 shows the result of a typical assay. Gal4 1–147 bound to DNA and served as a positive control. Specificity of the shifted band was demonstrated by the loss of the band when antibodies against Gal4 1–147 were added to the activated samples prior to the addition of the Gal4 oligonucleotide (Fig. 6, lanes 8 and 10). The Gal4/rtARNT$_{EX-QN}$, Gal4/rtARNT$_{QN}$, and Gal4/rtARNT$_{EX}$ proteins also produced gel shifts. These results are consistent with the finding that each protein exhibited transcriptional activity (Fig. 5A). In contrast, Gal4/rtARNT$_{EX-PST}$ and Gal4/rtARNT$_{PST}$ failed to shift the DNA containing the Gal4 binding site. These results suggest that the inability to detect transactivation activity in the PST-rich domain was due to reduced binding of the complex to DNA and not lack of TAD activity. Thus, the Gal4/rtARNT$_{EX-PST}$ protein had negative function at the level of DNA binding, just as observed when the domain was analyzed in the context of AHR-mediated signaling (Figs. 3 and 4). Since the Gal4 protein and AHR•ARNT complex bind DNA through distinct protein

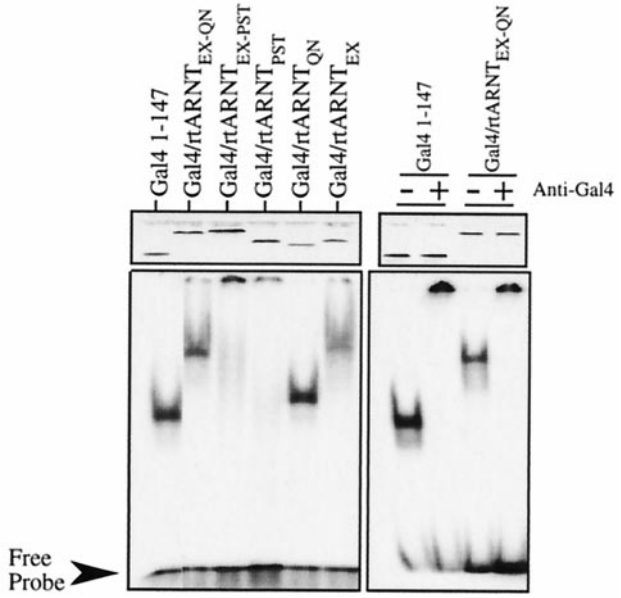

FIG. 6. Electrophoretic mobility shift analysis of Gal4/rtARNT protein. Each Gal4/rtARNT protein was produced in a coupled TNT reaction. Identical amounts of recombinant protein were subjected to EMSA with the Gal4 DNA binding domain as detailed in Materials and Methods. Shifted bands can be observed at different mobilities that correlate with the size of the Gal4/rtARNT protein. The specificity of the shifted bands is demonstrated in lanes 8 and 10, where the addition of anti-Gal4 antibody to the reaction resulted in loss of the band. The relative level of Gal4/rtARNT protein used in each reaction can be seen in the western blot at the top of the EMSA gel. These samples represent an aliquot of the identical reactions used for the EMSA that has been stained with the anti-Gal4 antibody.

domains, the ability of the PST-rich domain to affect binding is intriguing. Since the Gal4 proteins bind to DNA as a dimer [46], it is possible that the PST-rich domain disrupts dimerization. Alternatively, the PST-rich sequence may interfere directly with DNA binding of the dimer through masking of the sequence or misfolding of the protein.

Truncation of the PST-Rich C-Terminal Domain

It was next of interest to determine whether there were specific domains within the PST-rich region that contributed to the negative function of this sequence. Computer analysis of the 104-amino-acid C-terminal domain revealed several regions of interest (Fig. 7A). Overall, the sequence was dominated by β-sheets, numerous turn regions, and a lack of α-helices. In addition, the first 40 amino acids were hydrophilic, whereas the last 20 amino acids contained a region that appeared to be strongly hydrophobic. There were also four consensus motifs for PKC phosphorylation and one CK2 site (Fig. 7A). To assess the impact of these regions within the 104-amino-acid domain, several deletions were made (Fig. 7B). The first truncation removed the hydrophobic region identified in the final 20 amino acids and was designated $rtARNT_{\Delta 617}$. The second truncation was designed to conserve the hydrophilic region and three PKC sites present within the first 50 residues of the C-terminal domain and was designated $rtARNT_{\Delta 580}$. Each construct was transfected into type II cells, and the expression of P4501A1 was quantified as detailed for previous experiments. Figure 8A shows the western blot from a representative experiment in which each sample represents a single dish of transfected cells.

The results show that all of the transfected cells expressed a similar level of rtARNT protein that migrated at the expected molecular mass. Consistent with previous results (Fig. 3), type II cells transfected with $rtARNT_b$ or $rtARNT_{533}$ were capable of complementing AHR-mediated signaling, whereas transfection of $rtARNT_a$ resulted in minimal induction of P4501A1 expression. However, removal of 20 amino acids from the C-terminus of $rtARNT_a$ resulted in a protein ($rtARNT_{\Delta 617}$) that regained function in AHR-mediated signaling to 50% of the level of $rtARNT_b$ and 73% of the level of $rtARNT_{533}$ (Fig. 8C). Similar results were obtained in cells expressing the $rtARNT_{\Delta 580}$ protein, which functioned in AHR-mediated signaling to 75% of the level of $rtARNT_b$ and to nearly 100% of the level of $rtARNT_{533}$ (Fig. 8C). To confirm that these results were related to recovery of DNA binding of the rtARNT•AHR heterodimer, rtARNT protein was produced *in vitro* and quantified on western blots. Identical amounts of recombinant protein then were activated with type II cytosol as detailed and evaluated by EMSA (Fig. 8B). As observed in the complementation experiments, truncation of the C-terminal 20 amino acids partially restored the function of $rtARNT_a$. $rtARNT_{\Delta 617}$ produced a gel shift that was approximately 30% of that observed with $rtARNT_b$, but was 55% of the level observed with $rtARNT_{533}$. Similar results were observed with the $rtARNT_{\Delta 580}$, which resulted in XRE binding to 90% of the level of $rtARNT_{533}$. These results are consistent with the complementation experiments and show that truncation of the C-terminal domain restored the ability of the rtARNT•AHR complex to associate with the XRE. This suggests that the hydrophobic domain and not the PST-rich region is primarily responsible for the negative function of $rtARNT_a$.

CONCLUSIONS AND IMPLICATIONS

Recently, several bHLH/PAS proteins have been described that inhibit the functionality of bHLH/PAS heterodimers. One of the ARNT protein isoforms from rainbow trout, $rtARNT_a$, can bind to mAHR and function as a dominant negative regulator of AHR-mediated signaling [13]. mSIM2, on the other hand, appears to bind to ARNT in a nonfunctional heterodimer [30, 31]. In the case of $rtARNT_a$, negative function appears to involve sequestration of liganded AHR in a complex that does not bind DNA, while mSIM2 appears to suppress the transactivation of ARNT, but can also prevent ARNT from forming functional heterodimers with HIF-1α. The striking feature

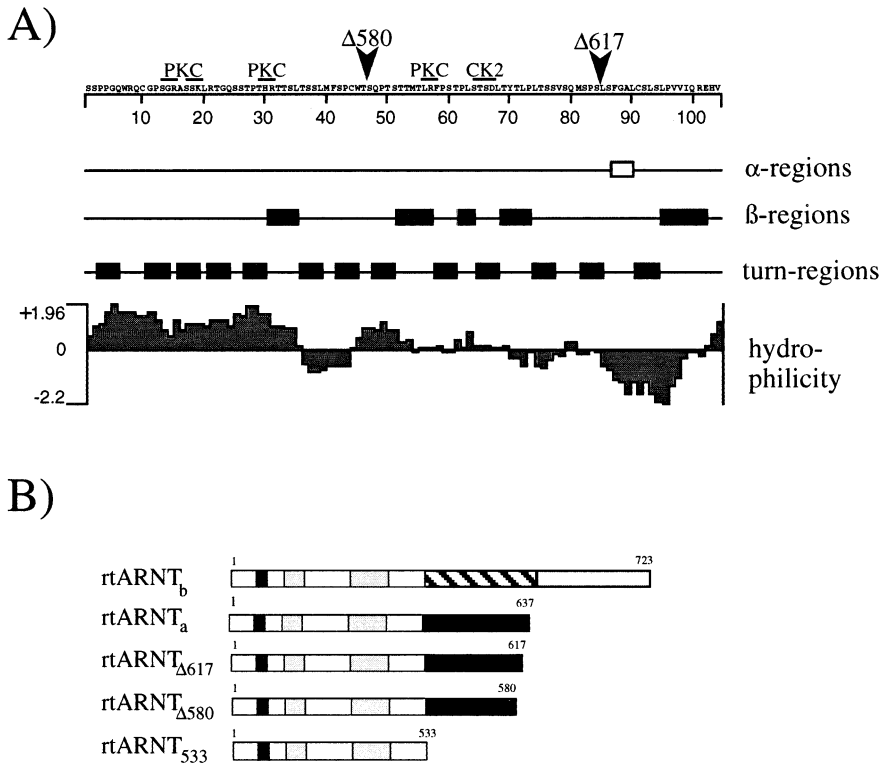

FIG. 7. Detailed analysis of PST-rich C-terminal domain of rtARNT$_a$. (A) The 104-amino-acid C-terminal domain of rtARNT$_a$ was analyzed for secondary structure as detailed in Materials and Methods. Boxed regions indicate areas predicted to be α-helix, β-sheet, or turn regions. Positive values predict areas that are hydrophilic and have a high probability of being on the surface of the protein. Consensus phosphorylation sites for protein kinase C (PKC) and casein kinase 2 (CK2) are overlined. The location of the C-terminal truncations are also indicated by the arrows. (B) Schematic diagram of the rtARNT constructs used to analyze the function of the C-terminal domain of rtARNT$_a$.

of both rtARNT$_a$ and mSIM2 function, however, is the fact that the C-terminal domains of these proteins appear to confer their negative function. Thus, studies were performed to functionally evaluate the C-terminal domains of rtARNT$_a$ with respect to AHR-mediated signaling. The power of the experiments detailed in this report is the evaluation of AHR-mediated signaling through analysis of changes in expression of the *endogenous CYP1A1* gene and direct correlation to the expression of different ARNT proteins.

The results show that the C-terminal domain structure of the functional rtARNT$_b$ protein is similar to mammalian ARNT and contains a potent TAD. In contrast, the C-terminus of rtARNT$_a$ appears to be responsible for the negative function of this protein. Indeed, truncation of the C-terminal 20 amino acids of rtARNT$_a$ restores function to rtARNT$_a$ in AHR-mediated signaling. In addition, expression of the C-terminal domain of rtARNT$_a$ in the context of mARNT, rtARNT$_b$, or Gal4 fusion proteins reduced function of these proteins at the level of DNA binding. Analysis of the 20-amino-acid domain responsible for the negative activity of rtARNT$_a$ shows that the region is hydrophobic and has a low probability of being on the surface of the protein. In addition, the sequence is not rich in PST residues (with respect to the rest of the C-terminal domain) and has minimal secondary structure. A search of GENBANK revealed no other proteins that contained this sequence. Thus, the amino acid sequence itself may not be as important as its hydrophobic nature and location in the C-terminal portion of the protein.

Functional diversity in the C-terminal domain of transcription factors appears to be a common theme. For example, alternative RNA splicing results in expression of a thyroid hormone receptor isoform (Trα2) with a divergent C-terminal domain that can repress TR activated gene expression through competition for DNA binding [47]. Phosphorylation and dephosphorylation of the C-terminal domain of TRα2 appear to regulate the activity of this protein. The transcriptional competence of B cell-specific transcription factor is determined by activating and inhibitory sequences in the PST-rich C-terminal domain of this protein that may be affected by changes in phosphorylation as well [48]. In contrast, one member of the nuclear factor 1 family of transcription factors, termed NF1-X, contains a novel C-terminal domain that appears to repress the DNA binding activity of NF1 heterodimers by the formation of non-functional heterodimers [49]. Interestingly, the expression of the NF1-X C-terminal domain on Gal4 fusion proteins also affects DNA binding just as reported here for the C-terminus of rtARNT$_a$. The precise mechanism whereby these factors inhibit DNA binding is not known and will likely require crystallographic analysis. However,

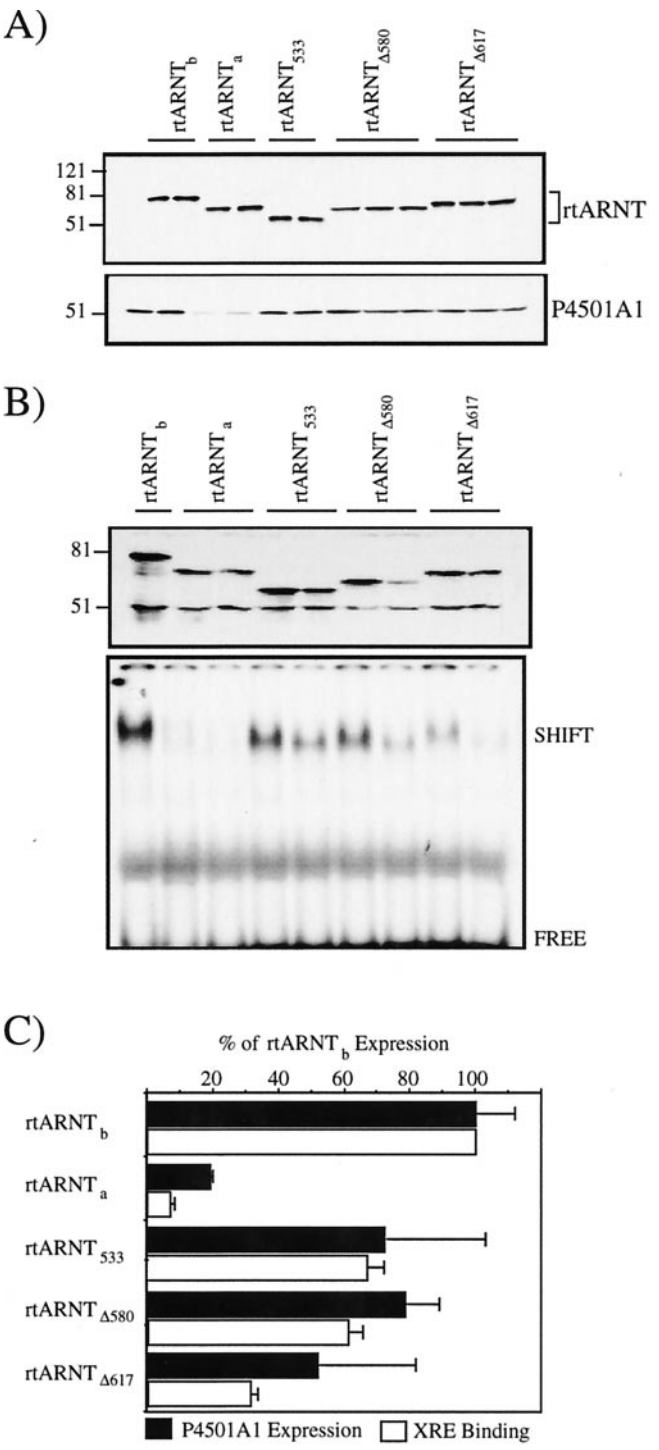

FIG. 8. Functional analysis of the C-terminal domain of rtARNT$_a$. (A) Western blot of P4501A1 expression in TCDD-treated type II cells expressing rtARNT proteins. Two to three plates of type II cells were transfected with the indicated constructs, treated with TCDD (1 nM) for 16 hr, and total cell lysates were prepared. Eighteen micrograms of each sample was subjected to denaturing gel electrophoresis and blotted to nitrocellulose. Duplicate blots were stained with either rt-84 IgG (1.0 μg/mL) or anti-P4501A1 IgG (1:500). Blots were then stained with GAR-HRP (1:10,000) and visualized by ECL. Molecular mass markers were β-galactosidase (121 kDa), BSA (81 kDa), and ovalbumin (51 kDa). (B) EMSA of rtARNT protein. One hundred micrograms of type II cytosol was combined with either 20 or 50 ng of the indicated rtARNT protein. Then samples were activated with TCDD (10 nM) for 2 hr at 30°, and EMSA was performed as detailed in Materials and Methods. The specifically shifted band associated with rtARNT•AHR•XRE complex is indicated. The western blot at the top of the EMSA represents an aliquot of the exact samples used for the EMSA stained with the rt-84 antibody as detailed in part A. Each pair of lanes represents use of 50 and 20 ng of the indicated ARNT protein, respectively. Molecular mass markers were BSA (81 kDa) and ovalbumin (51 kDa). (C) Composite of P4501A1 expression and XRE binding. The levels of P4501A1, rtARNT protein, and specifically shifted XRE were quantified by computer densitometry as detailed in Materials and Methods. The data are presented as the percentage of P4501A1 expression or XRE binding compared with that calculated for rtARNT$_b$ (100%). Each bar represents the mean ± SD of three independent samples.

based on the biochemical data, it is logical to hypothesize that the C-terminal end of rtARNT$_a$ causes a conformational change in the AHR•ARNT heterodimer that affects DNA binding. This hypothesis is supported by the finding that the immediate C-terminal domain of rtARNT$_a$ is hydrophobic and, therefore, likely to be inside the protein and not on the surface. Such a location may displace the basic region from the proper context or mask it completely. Displacement or masking of DNA binding domains would also explain why the C-terminal end of rtARNT$_a$ affects the binding of Gal4 complexes even though they bind DNA through different protein domains than AHR•ARNT complexes. However, because the Gal4 proteins bind to DNA as a dimer [46], it cannot be ruled out that the domain disrupts dimerization. These mechanisms are consistent with those proposed for the function of NF1-X [49].

The biological relevance of rtARNT$_a$ has not been resolved, and the presence of a mammalian homologue is unknown. Since the protein appears to have a negative function in AHR-mediated signaling, this protein may modulate the intensity of the response to AHR agonists. Alternatively, the known range of function of the ARNT protein is still expanding, and rtARNT$_a$ may interact with other bHLH/PAS proteins in positive or negative ways. The finding that functional diversity within the C-terminal domain is responsible for the negative action of this protein on AHR-mediated signaling is in agreement with the function of other negatively acting transcription factors and illustrates a common biological theme [30–32, 47–49]. The data in this report also highlight the fact that the C-terminal regions of bHLH/PAS proteins likely confer more functionality to the protein than just transactivation. Indeed, recent domain analysis of mSIM2 has shown that the C-terminal region represses the transactivation function of ARNT [30, 31]. Therefore, since the ARNT protein is utilized by numerous signaling systems [7, 9, 10, 15, 16, 27, 28, 31, 32] and appears to be essential to normal development [50, 51], experiments are in progress not only to evaluate the function of rtARNT$_a$ in non-AHR-mediated pathways (i.e. hypoxia), but to evaluate the expression of

this protein during key developmental time points. As more bHLH/PAS proteins are described, it is anticipated that analysis of C-terminal function will add to the complexity of bHLH/PAS protein signaling.

This project was supported, in part, by grants to R. S. P. from the National Institute of Environmental Health Sciences (Grant ES 08980) and the South Carolina Seagrant Consortium (Grant R/ER-12) and a STAR Graduate Fellowship to B. N. from the Environmental Protection Agency (Fellowship 915218–01).

References

1. Blackwell TK and Weintraub H, Differences and similarities in DNA-binding preferences of MyoD and E2A protein complexes revealed by binding site selection. *Science* **250:** 1104–1110, 1990.
2. Dolwick KM, Swanson HI and Bradfield CA, *In vitro* analysis of AH receptor domains involved in ligand-activated DNA recognition. *Proc Natl Acad Sci USA* **90:** 8566–8570, 1993.
3. Reisz-Porszasz S, Probst MR, Fukunaga BN and Hankinson O, Identification of functional domains of the aryl hydrocarbon receptor nuclear translocator protein (ARNT). *Mol Cell Biol* **14:** 6075–6086, 1994.
4. Lindebro MC, Poellinger L and Whitelaw ML, Protein-protein interaction via PAS domains: Role of the PAS domain in positive and negative regulation of the bHLH/PAS dioxin receptor-ARNT transcription factor complex. *EMBO J* **14:** 3528–3539, 1995.
5. Bacsi SG and Hankinson O, Functional characterization of DNA-binding domains of the subunits of the heterodimeric aryl hydrocarbon receptor complex imputing novel and canonical basic helix-loop-helix protein-DNA interactions. *J Biol Chem* **271:** 8843–8850, 1996.
6. Whitelaw ML, Gustafsson J-A and Poellinger L, Identification of transactivation and repression functions of the dioxin receptor and its basic helix-loop-helix/PAS partner factor ARNT: Inducible versus constitutive modes of regulation. *Mol Cell Biol* **14:** 8343–8355, 1994.
7. Wang GL, Jiang B-H, Rue EA and Semenza G, Hypoxia inducible factor-1 is a bHLH/PAS heterodimer regulated by cellular O_2 tension. *Proc Natl Acad Sci USA* **92:** 5510–5514, 1995.
8. Huang ZJ, Edery I and Robash M, PAS is a dimerization domain common to *Drosophila* period and several transcription factors. *Nature* **364:** 259–262, 1993.
9. Tian H, McKnight SL and Russell DW, Endothelial PAS domain protein 1 (EPAS1), a transcription factor selectively expressed in endothelial cells. *Genes Dev* **11:** 72–82, 1997.
10. Ema M, Taya S, Yokotani N, Sogawa K, Matsuda Y and Fujii-Kuriyama Y, A novel bHLH-PAS factor with close sequence similarity to hypoxia-inducible factor 1α regulates the *VEGF* expression and is potentially involved in lung and vascular development. *Proc Natl Acad Sci USA* **94:** 4273–4278, 1997.
11. Hirose K, Morita M, Ema M, Mimura J, Hamada H, Fuji H, Saijo Y, Gotoh O, Sogawa K and Fuji-Kuriyama Y, cDNA cloning and tissue-specific expression of a novel basic helix-loop-helix/PAS factor (ARNT) with close sequence similarity to the aryl hydrocarbon receptor nuclear translocator (ARNT). *Mol Cell Biol* **16:** 1706–1713, 1996.
12. Drutel G, Kathmann M, Heron A, Schwartz J-C and Arrang J-M, Cloning and selective expression in brain and kidney of ARNT2 homologous to the AH receptor nuclear translocator (ARNT). *Biochem Biophys Res Commun* **225:** 333–339, 1996.
13. Pollenz RS, Sullivan HR, Holmes J, Necela B and Peterson RE, Isolation and expression of cDNAs from rainbow trout (*Oncorhynchus mykiss*) that encodes two novel basic-helix-loop-helix/PER-ARNT-SIM (bHLH/PAS) proteins with distinct functions in the presence of the aryl hydrocarbon receptor. *J Biol Chem* **271:** 30886–30896, 1996.
14. Wilson CL, Thomsen J, Hoivik DJ, Wormke MT, Stanker L, Holtzapple C and Safe SH, Aryl hydrocarbon (AH) nonresponsiveness in estrogen receptor-negative MDA-MB-231 cells is associated with expression of a variant arnt protein. *Arch Biochem Biophys* **346:** 65–73, 1997.
15. Poland A and Knutson JC, 2,3,7,8-Tetrachlorodibenzo-*p*-dioxin and related aromatic hydrocarbons. Examination of the mechanism of toxicity. *Annu Rev Pharmacol Toxicol* **22:** 517–554, 1982.
16. Hankinson O, The aryl hydrocarbon receptor complex. *Annu Rev Pharmacol Toxicol* **35:** 307–340, 1995.
17. Whitlock JP Jr, Mechanistic aspects of dioxin action. *Chem Res Toxicol* **6:** 754–763, 1993.
18. Pollenz RS, The aryl-hydrocarbon receptor, but not the aryl-hydrocarbon receptor nuclear translocator protein, is rapidly depleted in hepatic and nonhepatic culture cells exposed to 2,3,7,8-tetrachlorodibenzo-*p*-dioxin. *Mol Pharmacol* **49:** 391–398, 1996.
19. Holmes JL and Pollenz RS, Determination of aryl hydocarbon receptor nuclear translocator protein concentration and subcellular localization in hepatic and nonhepatic cell culture lines: Development of quantitative western blotting protocols for calculation of aryl hydrocarbon receptor and aryl hydrocarbon receptor nuclear translocator protein in total cell lysates. *Mol Pharmacol* **52:** 202–211, 1997.
20. Whitelaw M, Pongratz I, Wilhelmsson A, Gustafsson JA and Poellinger L, Ligand-dependent recruitment of the Arnt coregulator determines DNA recognition by the dioxin receptor. *Mol Cell Biol* **13:** 2504–2514, 1993.
21. Fujisawa-Sehara A, Sogawa K, Yamane M and Fujii-Kuriyama Y, Characterization of xenobiotic responsive elements upstream from the drug-metabolizing cytochrome P-450c gene: A similarity to glucocorticoid regulatory elements. *Nucleic Acids Res* **15:** 4179–4191, 1987.
22. Denison M, Fisher J and Whitlock JP Jr, The DNA recognition site for the dioxin-AH receptor complex. *J Biol Chem* **263:** 17221–17224, 1988.
23. Li H, Ko HP and Whitlock JP Jr, Induction of phosphoglycerate kinase 1 gene expression by hypoxia. Roles of Arnt and HIF1α. *J Biol Chem* **271:** 21262–21267, 1996.
24. Jiang BH, Rue E, Wang GL, Roe R and Semenza GL, Dimerization, DNA binding, and transactivation properties of the hypoxia-inducible factor 1. *J Biol Chem* **271:** 17771–17778, 1996.
25. Gradin K, McGuire J, Wenger RH, Kvietikova I, Whitelaw ML, Toftgard R, Tora L, Gassman M and Poellinger L, Functional interference between hypoxia and dioxin signal transduction pathways: Competition for recruitment of the ARNT transcription factor. *Mol Cell Biol* **16:** 5221–5231, 1996.
26. Wood SW, Gleadle JM, Pugh CW, Hankinson O and Radcliffe PJ, The role of the aryl hydrocarbon receptor nuclear translocator (ARNT) in hypoxic induction of gene expression. *J Biol Chem* **271:** 15117–15123, 1996.
27. Antonsson C, Arulampalam V, Whitelaw ML, Pettersson S and Poellinger L, Constitutive function of the basic helix-loop-helix/PAS factor Arnt: Regulation of target promoters via the E box motif. *J Biol Chem* **270:** 13968–13972, 1995.
28. Sogawa K, Nakano R, Kobayashi A, Kikuchi Y, Ohe N, Matsushita N and Fuji-Kuriyama Y, Possible function of AH receptor nuclear translocator (ARNT) homodimer in transcriptional regulation. *Proc Natl Acad Sci USA* **92:** 1936–1940, 1995.

29. Swanson HI, Chan WK and Bradfield CA, DNA binding specificities and pairing rules of the Ah receptor, ARNT, and SIM proteins. *J Biol Chem* **270:** 26292–26302, 1995.
30. Ema M, Morita M, Ikawa S, Tanaka M, Matsuda Y, Gotoh O, Saijoh Y, Fujii H, Hamada H, Kikuchi Y and Fuji-Kuriyama Y, Two new members of the murine *Sim* gene family are transcriptional repressors and show different expression patterns during mouse embryogenesis. *Mol Cell Biol* **16:** 5865–5875, 1996.
31. Moffett P, Reece M and Pelletier J, The murine *Sim-2* gene product inhibits transcription by active repression and functional interference. *Mol Cell Biol* **17:** 4933–4947, 1997.
32. Probst MR, Fan CM, Tessier-Lavigne M and Hankinson O, Two murine homologs of the *Drosophila* single-minded protein that interact with the mouse aryl hydrocarbon receptor nuclear translocator protein. *J Biol Chem* **272:** 4451–4457, 1997.
33. Jain S, Dolwick KM, Schmidt LV and Bradfield CA, Potent transactivation domains of the AH receptor and the AH receptor nuclear translocator map to their carboxy termini. *J Biol Chem* **269:** 31518–31524, 1994.
34. Li H, Dong L and Whitlock JP Jr, Transcriptional activation function of the mouse Ah receptor nuclear translocator. *J Biol Chem* **269:** 28098–28105, 1994.
35. Rowlands JC, McEwan IJ and Gustafsson J-Å, *Trans*-activation by the human aryl hydrocarbon receptor and aryl hydrocarbon receptor nuclear translocator proteins: Direct interactions with basal transcription factors. *Mol Pharmacol* **50:** 538–548, 1996.
36. Corton JC, Moreno ES, Hovis SM, Leonard LS, Gaido KW, Joyce MM and Kennett SB, Identification of a cell-specific transcription activation domain within the human AH receptor nuclear translocator. *Toxicol Appl Pharmacol* **139:** 272–280, 1996.
37. Franks RG and Crews ST, Transcriptional activation domains of the single-minded bHLH protein are required for CNS midline cell development. *Mech Dev* **45:** 269–277, 1994.
38. Pollenz RS, Sattler CA and Poland A, The aryl hydrocarbon receptor and aryl hydrocarbon receptor nuclear translocator protein show distinct subcellular localizations in Hepa 1c1c7 cells by immunofluorescence microscopy. *Mol Pharmacol* **45:** 428–438, 1994.
39. Sadowski I and Ptashne M, A vector for expressing GAL4(1–147) fusions in mammalian cells. *Nucleic Acids Res* **17:** 7539, 1989.
40. Sambrook J, Fritsch EF and Maniatis T, *Molecular Cloning. A Laboratory Manual*. Cold Spring Harbor Laboratory Press, Cold Spring Harbor, NY, 1989.
41. Shen ES and Whitlock JP Jr, Protein-DNA interactions at the dioxin-responsive promoter. *J Biol Chem* **267:** 6815–6819, 1992.
42. Giniger E, Varnum SM and Ptashne M, Specific DNA binding of Gal4, a positive regulatory protein of yeast. *Cell* **40:** 767–774, 1985.
43. Bram RJ, Lue NF and Kornberg RD, A Gal family of upstream activating sequences in yeast: Roles in both induction and repression of transcription. *EMBO J* **5:** 603–608, 1986.
44. Pollenz RS and Necela B, Characterization of two continuous cell lines derived from *Oncorhynchus mykiss* for models of aryl-hydrocarbon-receptor-mediated signal transduction. Direct comparison to the mammalian Hepa-1c1c7 cell line. *Aquat Toxicol* **41:** 31–49, 1998.
45. Ko HP, Okino ST, Ma Q and Whitlock JP Jr, Dioxin-induced *CYP1A1* transcription *in vivo*: The aromatic hydrocarbon receptor mediates transactivation, enhancer-promoter communication, and changes in chromatin structure. *Mol Cell Biol* **16:** 430–436, 1996.
46. Carey M, Kakidani H, Leatherwood J, Mostashari F and Ptashne M, An amino-terminal fragment of GAL4 binds DNA as a dimer. *J Mol Biol* **209:** 423–432, 1989.
47. Katz D, Reginato M and Lazar M, Functional regulation of thyroid hormone receptor variant TRα2 by phosphorylation. *Mol Cell Biol* **15:** 2341–2348, 1995.
48. Dorfler P and Busslinger M, C-terminal activating and inhibitory domains determine the transactivation potential of BSAP (Pax-5), Pax-2 and Pax-8. *EMBO J* **15:** 1971–1982, 1996.
49. Roulet E, Armentero MT, Krey G, Corthésy B, Dreyer C, Mermod N and Wahli W, Regulation of the DNA-binding and transcriptional activities of *Xenopus laevis* NFI-X by a novel C-terminal domain. *Mol Cell Biol* **15:** 5552–5562, 1995.
50. Maltepe E, Schmidt JV, Baunoch D, Bradfield CA and Simon MC, Abnormal angiogenesis and responses to glucose and oxygen deprivation in mice lacking the ARNT protein. *Nature* **386:** 403–407, 1997.
51. Kozak KR, Abbott B and Hankinson O, ARNT-deficient mice and placental differentiation. *Dev Biol* **191:** 297–305, 1997.